ϕ −74.5 (d-p) for CF_3^a ($^3J_{FF}$ = 5.4 Hz and $^4J_{FF_{eq}}$ = 9.3 Hz) and ϕ −141.0 (mult) for CF^b. The mass spectrum shows a molecular ion at *m/e* 257 (less than 1% of base peak), with other fragments of *m/e* 127 (SF_5^+, 62%), 100 (CF_3CF^+, 100%), 89 (SF_3^+, 43%), 69 (CF_3^+, 58%), and 30 (NO^+, 58%).

Anal. Calcd for $CF_3CF(NO)SF_5$: N, 5.45; F, 66.52. Found: N, 6.51; F, 66.2.

$CF_3^aCF^b(NO)OCF_2^cCF_3^d$. A stainless-steel 75-mL Hoke vessel, fitted with a stainless-steel Hoke valve and containing 2–3 g (13–19 mmol) of anhydrous CsF and several $^5/_{32}$-in stainless-steel balls, was loaded with CF_2=$CFOCF_2CF_3$ (4.25 mmol), NO (5 mmol), NF_3O (2.5 mmol), and CH_3CN (3 mL) at −196 °C. After warming to ambient temperature, the bomb was shaken mechanically for 5 days. Upon distillation, the trap held at −116 °C contained 2.7 mmol of an intensly blue liquid. The liquid was greater than 91% pure (overall yield 58%) as determined by gas chromatographic methods (24-ft column; Kel-F No. 3 oil on Chromosorb P). This new nitroso compound, a deep blue liquid and gas, has a vapor pressure of 314 mm at 0 °C. Vapor-phase infrared spectrum: 1606 m, 1384 m, 1346 s, 1248 vs, 1253 s, 1179 vs, 1142 s, 1099 s, 1056 m, 967 w, 841 w, 749 m, 610 w cm^{-1}. The ^{19}F NMR spectrum, recorded as a liquid under autogeneous pressure at ambient temperature, consists of a broad singlet at ϕ −82.6 due to CF_3^a, a doublet of multiplets at ϕ −86.2 ($^4J_{FF}$ = 15 Hz) due to CF_2^c, a multiplet at ϕ −89.2 due to CF_3^d, and a triplet at ϕ −129.3 ($^4J_{FF}$ = 15 Hz) due to CF^b. The mass spectrum shows a molecular ion at *m/e* 265 (<1% of the base peak). Other fragments occur at *m/e* 235 ($C_4F_9O^+$), 130 ($C_2F_4NO^+$), 119 ($C_2F_5^+$), 111 ($C_2F_3NO^+$), 100 ($C_2F_4^+$), 97 ($C_2F_3O^+$), and 69 (CF_3^+). Molecular weight: found by *PVT* methods, 258; calcd, 265.

Acknowledgment is expressed to the donors of the Petroleum Research Fund, administered by the American Chemical Society, to the National Science Foundation (Grant CHE-8100156), and to the Air Force Office of Scientific Research (Grant 82-0247) for support of this research. Drs. David England and Carl Krespan of Du Pont are thanked for the vinyl ether. Dr. Gary Knerr obtained the ^{19}F NMR and mass spectra.

Registry No. $CF_3CF(NO)(CF_2)_4CF_3$, 92844-16-1; NO, 10102-43-9; NF_3O, 13847-65-9; CF_2=$CF(CF_2)_4CF_3$, 355-63-5; $CF_3CF(NO)SF_5$, 92844-17-2; CF_2=$CFSF_5$, 1186-51-2; $CF_3CF(NO)OCF_2CF_3$, 92844-18-3; CF_2=$CFOCF_2CF_3$, 10493-43-3; FNO, 7789-25-5.

Contribution from the Department of Chemistry, University of Delaware, Newark, Delaware 19716

The Effect of X^- = Cl^-, Br^-, I^- on the Kinetics of the Arbuzov Rearrangement Involving $[CpCo(dppe)X]^+$ and $P(OR)_3$ (R = Me, Et)

SHAYNE J. LANDON and THOMAS B. BRILL*

Received April 9, 1984

Rate constants and equilibrium and transition-state data for the reaction of $[CpCo(dppe)X]^+$ (X^- = Cl^-, Br^-, I^-) (**1**) with $P(OR)_3$ (R = Me, Et) to produce $\{CpCo(dppe)[P(O)(OR)_2]\}^+$ (**3**) and RX have been acquired by ^1H NMR spectroscopy. The rate of the overall reaction (X^- = I^- > Br^- > Cl^-) is traceable to the trend of X^- as a leaving group from the Co(III) center in the preequilibrium step that leads to the intermediate complex $[CpCo(dppe)P(OMe)_3]^{2+}$ (**2**). The rate of the dealkylation of **2** to form **3** is only moderately sensitive to X^-, suggesting that nucleophilicity of X^- plays a subordinate role. ΔH^* and ΔS^* for **2** → **3** are monotonically related and give an isokinetic temperature of −45 °C. ΔS^* is large and positive owing probably to the fact that ions having 2+ and 1− charge come together in the transition state. The entropy factor strongly influences the reaction rate above −45 °C. A comparison of the kinetic parameters for the Arbuzov reaction involving a transition-metal center vs. an alkyl center helps explain why the rearrangement is more facile in the former.

Introduction

The well-known Arbuzov (or Michaelis–Arbuzov) reaction[1] in which an alkyl phosphite and an alkyl halide react to form an alkyl phosphonate with alkyl transfer has precedence in transition-metal chemistry. In place of the alkyl halide, certain transition-metal–halide complexes undergo reaction 1 yielding,

$$L_nM\text{–}X + P(OR)_3 \rightarrow L_nMP(O)(OR)_2 + RX \quad (1)$$

ultimately, a transition-metal–phosphonate complex as one of the final products.[2] An ionic mechanism has been put forth for this rearrangement in which $P(OR)_3$ first displaces the X^- and then is attacked by X^-, liberating RX and the phosphonate complex.[3–6] Dealkylation of phosphite ligands by a radical pathway also occurs and to date has arisen following metal–metal bond homolysis in the presence of $P(OR)_3$.[7–9]

In recent studies our attention has focused on fully characterizing the ionic mechanism.[2,5] A class of metal–halide cations having the general formula $[CpCo(L\frown L)X]^+$ as BF_4^- salts satisfactorily probe several features of this reaction.[10] $L\frown L$ is a bidentate chelate ligand, and X^- is a halide ligand. The details of the reaction between $[CpCo(dppe)I]^+$ and $P(OMe)_3$ were established by ^1H and ^{31}P NMR spectroscopy in $CDCl_3$ solution.[5] The essential constituents and the mechanism are summarized in Figure 1. The final step, k_2, is rate determining, or **2** would not have been detected.

(1) For reviews see: (a) Bhattacharya, A. K.; Thyagarjan, G. *Chem. Rev.* **1981**, *81*, 415. (b) Kirby, A. J.; Warren, S. G. "The Organic Chemistry of Phosphorus"; Elsevier: New York, 1967; p 67. (c) Harvey, R. G.; DeSombre, E. R. *Top. Phosphorus Chem.* **1964**, *1*, 57. (d) Hudson, R. F. "Structure and Mechanism in Organo-phosphorus Chemistry"; Academic Press: New York, 1965; p 135. (e) Arbuzov, A. E. *Pure Appl. Chem.* **1964**, *9*, 307.

(2) Landon, S. J.; Brill, T. B. *Inorg. Chem.* **1984**, *23*, 1266. Brill, T. B.; Landon, S. J. *Chem. Rev.*, in press.

(3) Haines, R. J.; DuPreez, A. L.; Marais, I. L. *J. Organomet. Chem.* **1971**, *28*, 405.

(4) Trogler, W. C.; Epps, L. A.; Marzilli, L. G. *Inorg. Chem.* **1975**, *14*, 2748.

(5) Landon, S. J.; Brill, T. B. *J. Am. Chem. Soc.* **1982**, *104*, 6571.

(6) Towle, D. K.; Landon, S. J.; Brill, T. B.; Tulip, T. H. *Organometallics* **1982**, *1*, 295.

(7) Goh, L.-Y.; D'Aniello, M. J.; Slater, S.; Muetterties, E. L.; Tavanaiepour, I.; Chang, M. I.; Fredrich, M. F.; Day, V. W. *Inorg. Chem.* **1979**, *18*, 192.

(8) Howell, J. A. S.; Rowan, A. J. *J. Chem. Soc., Dalton Trans.* **1980**, 1845. Howell, J. A. S.; Rowan, A. J.; Snell, M. S. *J. Chem. Soc., Dalton Trans.* **1981**, 325.

(9) Wayland, B. B.; Woods, B. A. *J. Chem. Soc., Chem. Commun.* **1981**, 475.

(10) Abbreviations used: Cp = η^5-C_5H_5, dppe = 1,2-bis(diphenylphosphino)ethane, Ph = C_6H_5, Me = CH_3, Et = CH_3CH_2; b = broad, m = multiplet, s = singlet, t = triplet, q = quartet.

0020-1669/84/1323-4177$01.50/0

Table I. Equilibrium and Rate Constant Data in Acetone-d_6 for the Reactions in Figure 1[a]

	T, °C				
X^-	0	10	20	30	40
			a. k_{obsd}, L mol^{-1} s^{-1}		
Cl^-			1.1 (0.1) × 10^{-2}	3.5 (0.15) × 10^{-2}	5.7 (0.5) × 10^{-2}
Br^-		1.6 (0.05) × 10^{-1}	2.4 (0.3) × 10^{-1}	3.1 (0.3)	
I^-	3.6 (0.3) × 10^{-2}	6.3 (0.3) × 10^{-1}	7.6 (0.3) × 10^{-1}		
			b. K_{eq}		
Cl^-			1.2 (0.1) × 10^{-3}	1.1 (0.1) × 10^{-3}	3.2 (0.4) × 10^{-4}
Br^-		8.3 (1) × 10^{-2}	2.7 (0.4) × 10^{-2}	5.3 (0.8) × 10^{-2}	
I^-	7.3 (1.5) × 10^{-2}	3.6 (0.3) × 10^{-1}	1.3 (0.1) × 10^{-1}		
			c. k_2, L mol^{-1} s^{-1}		
Cl^-			9.2 (0.9)	3.2 (0.3) × 10	1.8 (0.2) × 10^2
Br^-		1.9 (0.2)	8.7 (1)	5.9 (0.7) × 10	
I^-	4.9 (0.4) × 10^{-1}	1.75 (0.15)	5.9 (0.5) × 10		

[a] Parenthetical numbers are the errors estimated from the standard deviation.

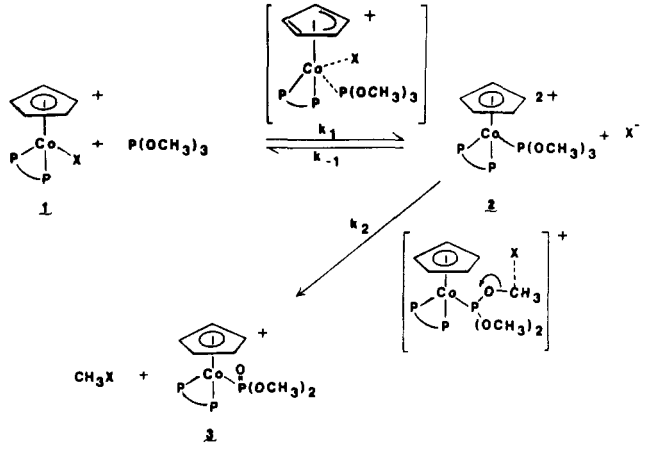

Figure 1. Ionic mechanism of the Arbuzov reaction in a transition-metal complex. Complexes drawn by the arrows are possible transition states.

Complex **2** can be isolated in the absence of nucleophiles.[2] The rate of conversion of **1** to **3** occurs qualitatively in the order $X^- = I^- > Br^- > Cl^-$, which is also the order found for the classical Arbuzov reaction involving alkyl halides.[11,12]

X^- might influence the rate of the reaction in several ways. The ability of $P(OMe)_3$ to displace X^- from the coordination sphere affects the equilibrium constant $K_{eq} = k_1/k_{-1}$. Thus the Co–X bond strength is a factor. In the second step of the reaction, the ability of X^- to dealkylate the phosphite ligand is related to the nucleophilicity of X^-. Because ions are involved, ion pairing and solvation differences also probably influence the entropy change and in turn the rate of the overall reaction.

Comprehensive insight into the transition-metal Arbuzov reaction occurring by the ionic mechanism emerges from a study of the individual steps in Figure 1 when $X^- = Cl^-$, Br^-, and I^-. Such a study at various temperatures was undertaken here by ^1H NMR spectroscopy. The results reveal how the halide ion controls the rate of the reaction and why the Arbuzov rearrangement involving a transition-metal complex usually occurs at a faster rate than the classical reaction.

Results

Several features of the ^1H NMR spectrum are useful for diagnosing the important aspects of this reaction, but the Cp region is straightforwardly analyzed because a sharp singlet appears for each complex. Complete spectra appear elsewhere.[2] The Cp protons of the dication, **2**, are least shielded and produce a signal at 6.02–6.15 ppm that depends slightly on X^-. Of course, δ_{Cp} (ppm) for $[CpCo(dppe)X](BF_4)$ depends markedly on X^-: 5.57, Cl^-; 5.62, Br^-; 5.79, I^-. The Cp signal for **3** is the most shielded and occurs at 5.50 ppm. Because of ion pairing, changes in the anion, such as from BF_4^- to PF_6^-, also affect the chemical shifts of these cations.

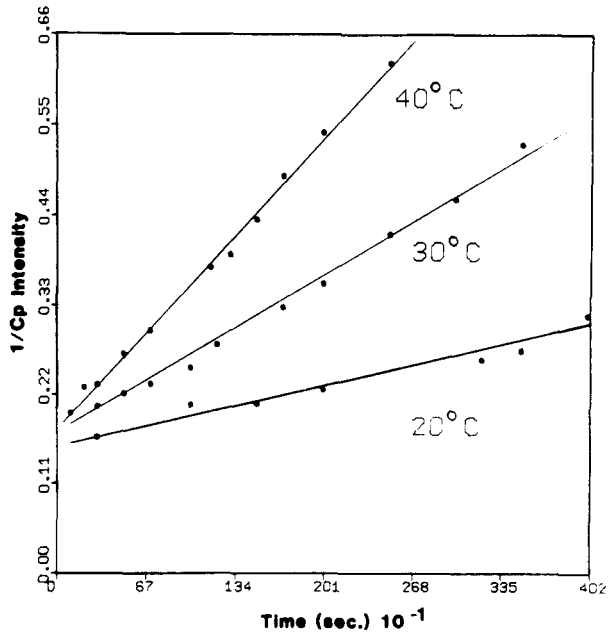

Figure 2. Second-order rate constant plots for k_{obsd} when $X^- = Cl^-$. The Cp signal intensity is proportional to concentration.

Equation 2 was established previously[5] for the overall reaction in Figure 1. Thus, when $[\mathbf{1}]_{init} = [P(OR)_3]_{init}$, a plot of $[\mathbf{1}]^{-1}$ vs. time is linear and the slope gives k_{obsd}. Figure 2

$$-d[\mathbf{1}]/dt = k_{obsd}[\mathbf{1}][P(OR)_3] \quad (2)$$

shows the rate data for $X^- = Cl^-$ and is representative of the equivalent data for Br^- and I^-. Table Ia summarizes the values of k_{obsd} at three temperatures for each halide ion.

It is readily shown from Figure 1 that $k_{obsd} = K_{eq}k_2$. K_{eq} can be calculated from the relative intensity of the Cp signals in **1** and **2**. $K_{eq} = ([\mathbf{2}]/[\mathbf{1}])^2$, and the values appear in Table Ib. K_{eq} was observed to be relatively constant and [**2**] relatively unchanged[5] through the middle stage (20–70% completion) of the reaction. From the experimental values of k_{obsd} and K_{eq}, k_2 can be determined in each case (Table Ic).

Arrhenius plots were constructed for the final step (k_2) in Figure 1 in order to determine the activation energy, E_a, and the frequency factor, A, for dealkylation. The enthalpy change,

(11) Laughlin, R. G.; Muratova, A. A.; Konnova, T. I.; Feoktistova, T.; Levkova, L. N. *J. Gen. Chem. USSR (Engl. Transl.)* **1960**, *30*, 2606.
(12) Pudovik, A. N.; Muratova, A. A.; Konnova, T. I.; Feoktistova, T.; Levkova, L N. *J. Gen. Chem. USSR (Engl. Transl.)* **1960**, *30*, 2606.

Table II. Rate and Equilibrium Data at 20 °C for the Reaction of $[CpCo(dppe)I]BF_4$ with $P(OR)_3$[a]

R	k_{obsd}, L mol^{-1} s^{-1}	K_{eq}	k_2, L mol^{-1} s^{-1}
Me	7.6 (0.3) × 10^{-1}	1.3 (0.1) × 10^{-1}	5.9 (0.5) × 10
Et	3.4 (0.3) × 10^{-4}	4.0 (0.3) × 10^{-2}	8.4 (0.6) × 10^{-3}

[a] See footnote *a* in Table I.

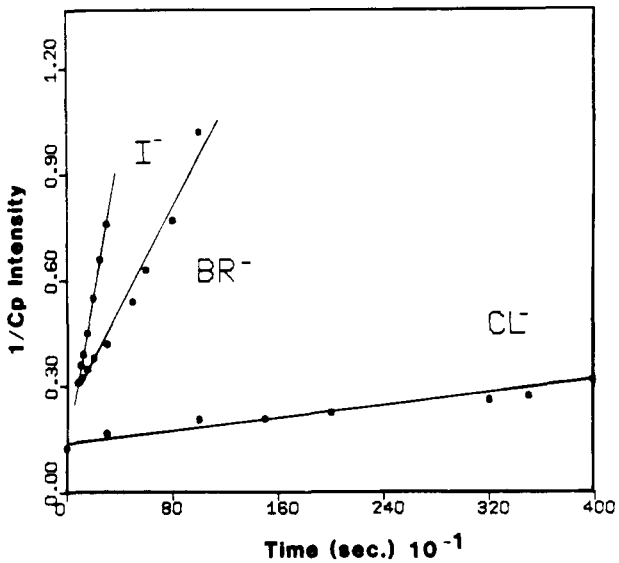

Figure 3. Plot of the rate constant data (k_{obsd}) at 20 °C for X^- = Cl^-, Br^-, and I^-. The Cp signal intensity is proportional to concentration.

$\Delta H^{\ddagger}$, and entropy change, $\Delta S^{\ddagger}$, of activation were calculated for each reaction at 20 °C from eq 3 and 4.[13] Table II contains these parameters.

$$\Delta H^{\ddagger} = E_a - RT \quad (3)$$

$$\Delta S^{\ddagger} = R(\ln A - ekT/h) \quad (4)$$

Discussion

The rate of conversion of **1** to **3**, subjectively observed previously[2] to follow the order $X^- = I^- > Br^- > Cl^-$ at room temperature, is now quantitatively supported by Figure 3 and the values of k_{obsd} at 20 °C in Table Ia. The origin of the difference in the overall reaction rates is traceable to the preequilibrium step where K_{eq} (Table Ib) at 20 °C suggests that $k_1(Cl^-) < k_1(Br^-) < k_1(I^-)$. The Co–X bond strength is probably the largest single determinant of k_1. Indeed, the order of k_1 coincides with the order of X^- as a leaving group from a Co(III) center.[14] Further support for the contribution of K_{eq} to the overall reaction rate stems from experiments in which $[(C_4H_9)_4N]X$ salts were added to **2**. Figure 4 shows the ^1H NMR spectra of the Cp region after 100 s at 0 °C following the addition of X^- to **2**. In each case, **1** appears before **3** and, in accordance with the trend in K_{eq}, $k_{-1}(Cl^-) > k_{-1}(Br^-) > k_{-1}(I^-)$.

The large effect of X^- on the equilibrium step contrasts with its feeble influence on k_2 according to the values in Table Ic at 20 °C. We are led to conclude that the nucleophilicity of these anions in the second step plays a relatively lesser role in the rate of the overall reaction. The conventional interpretation of the influence of X^- on the Arbuzov rearrangement involving RX and $P(OR)_3$ holds that the nucleophilicity of X^- controls the rate.[1,11,12] Although large differences in nucleophilicity do affect the reaction rate and pathway,[15] the differences among Cl^-, Br^-, and I^- are not a major factor in the rate of the transition-metal Arbuzov reaction and possibly not even in the classical reaction.[16]

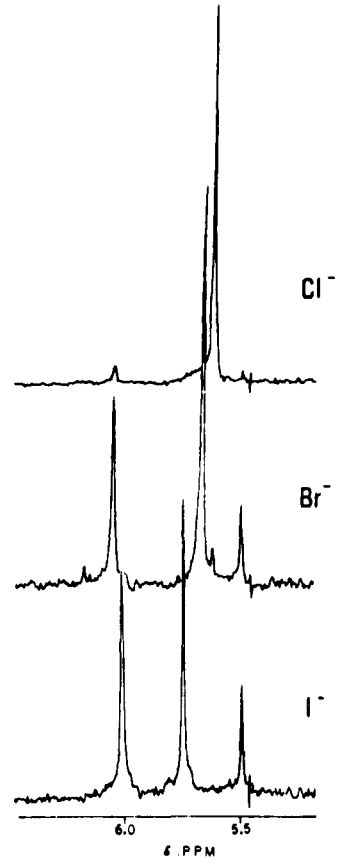

Figure 4. ^1H NMR spectra of the Cp region 100 s after the addition of $[(C_4H_9)_4N]X$ ($X^- = Cl^-$, Br^-, I^-) to **2** (0 °C). The spectra show that for Cl^-, **2** converts mostly to **1** so that the steady-state concentration of **2** is small. K_{eq} for Br^- and I^- is such that [**2**] is substantially larger, allowing the formation of **3** at a faster rate.

Table III. Activation-State Parameters for k_2[a]

X^-	$\Delta H^{\ddagger}$, kcal mol^{-1}	$\Delta S^{\ddagger}$, eu
Cl^-	29 (3)	78 (6)
Br^-	33 (4)	94 (9)
I^-	26 (1)	70 (5)

[a] See footnote *a* in Table I.

It is noteworthy that the susceptibility of the α-carbon atom of the phosphite ester to nucleophilic attack does strongly affect the rate of the dealkylation. For instance, when $P(OEt)_3$ replaces $P(OMe)_3$ as a reactant with $[CpCo(dppe)I]^+$ in Figure 1, k_2 (Table II) is much less because of the reduced positive charge on the α-carbon atoms of $P(OEt)_3$. K_{eq} is also smaller, perhaps because of the greater spacial demand of $P(OEt)_3$ compared to that of $P(OMe)_3$.

The activation parameters for dealkylation (k_2) appear in Table III. The large positive entropies of activation are probably associated with the fact that a substantial reduction of the net ionic charge occurs during the formation of the transition state. Furthermore, acetone is less comfortable accommodating highly ionic species than is, e.g., H_2O and should favor transition states that reduce the ionic strength. It is not obvious why substantial differences exist in $\Delta H^{\ddagger}$ and $\Delta S^{\ddagger}$ for this series of halide ions, but sharp differences are also

(13) Wilkins, R. G. "The Study of Kinetics and Mechanism of Reactions of Transition Metal Complexes"; Allyn and Bacon: Boston, 1974; p 80.
(14) Langford, C. H. *Inorg. Chem.* **1965**, *4*, 265.
(15) Lewis, E. S.; Hamp, D. *J. Org. Chem.* **1983**, *48*, 2025.
(16) Hudson, H. R.; Kow, A. T. C.; Henrick, K. In "Organophosphorus Chemistry"; Quin, L. D., Verkade, J. G., Eds.; American Chemical Society: Washington, DC, 1981; ACS Symp. Ser. No. 171, p 517.

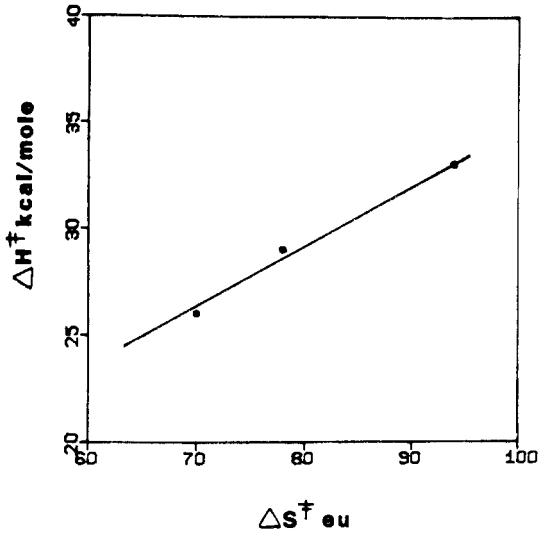

Figure 5. Correlation of $\Delta H^{\ddagger}$ and $\Delta S^{\ddagger}$ for the dealkylation step, k_2.

found in other reactions in which similar closely related variations have been made.[17] An important observation is that $\Delta H^{\ddagger}$ and $\Delta S^{\ddagger}$ linearly correlate (Figure 5), which gives strong evidence of a common mechanism for dealkylation of the phosphito ligand by Cl^-, Br^-, and I^- despite the range of values for $\Delta H^{\ddagger}$ and $\Delta S^{\ddagger}$. The slope of the line in Figure 5 yields an isokinetic temperature of about −45 °C. At this temperature all three dealkylation reactions occur at the same rate. Above −45 °C, $\Delta S^{\ddagger}$ more strongly influences the rate while $\Delta H^{\ddagger}$ would dominate below −45 °C. Thus the reaction rate is governed more by solvent ($\Delta S^{\ddagger}$) than by electronic ($\Delta H^{\ddagger}$) effects at room temperature. Such behavior could emanate from the fact that ions are produced and consumed in the nonaqueous environment, causing ion pairing and electrostriction to influence the formation of the transition state. Ion pairing is extensive in solutions of ions such as these.[18]

Comparison of the transition-metal-based Arbuzov reaction with the classical reaction is informative. Unlike the transition-metal reaction, dealkylation of the alkoxyphosphonium ion $[R'P(OR)_3]^+$ (R = organic groups) by nucleophiles usually requires heating for an extended period of time.[1] Although the kinetic data are limited, the reaction of $[R'P(OR)_3]^+$ (R′ = Me and R = neopentyl) with Br^- and I^- at 33 °C in $CDCl_3$ has been studied.[16] The rate constants for the step equivalent to k_2 in Figure 1 are smaller than those in the Table Ic by a factor of about 10^5. Thus the transition-metal-containing fragment is important for accelerating the conversion of a phosphite to a phosphonate. $\Delta H^{\ddagger}$ and $\Delta S^{\ddagger}$ data (two temperatures, no stated errors) are available for the classical reaction.[16] The values of $\Delta H^{\ddagger}$ for the conversion of $[Ph_2MeP(O\text{–neopentyl})]^+$ to $Ph_2MeP(O)$ by Cl^-, Br^-, and I^- range from 27 to 30 kcal mol^{-1}. This range compares with that of $\Delta H^{\ddagger}$ in Table III of 26–33 kcal mol^{-1}. The range of $\Delta S^{\ddagger}$ for this alkoxyphosphonium ion reacting with X^- is −1 to 9 eu. On the average, while the $\Delta H^{\ddagger}$ values are similar in the two systems, $\Delta S^{\ddagger}$ is vastly more positive for the transition-metal–phosphite complexes, which helps explain why dealkylation of the phosphite ligand occurs more rapidly. From an electronic point of view, the increased positive charge on the ester carbon of a phosphite ligand bound to an electropositive transition-metal center accentuates its susceptibility to nucleophilic attack. The large positive values of $\Delta S^{\ddagger}$ for the transition-metal complexes are probably related to the fact that species of 2+ and 1− charges come together in the activated complex whereas in the conventional Arbuzov reaction involving aliphatic substituents the charges are 1+ and 1−. As expected, the rate of this transition-metal Arbuzov reaction is strongly influenced by the choice of the solvent and the counteranion for $[CpCo(dppe)X]^+$.

Experimental Section

Synthesis. Reagent grade $CDCl_3$ and CH_3CN were purified by standard methods. $P(OR)_3$ (R = Me, Et) was distilled under N_2 prior to use. $CpCo(CO)_2$ (Strem) was used as received. $CpCoI_2(CO)$,[19] $[CpCo(dppe)X](BF_4)$ (X^- = Cl^-, Br^-, I^-),[2] and $\{CpCo(dppe)[P(OMe)_3]\}(PF_6)_2$[2] were prepared as described elsewhere. Melting points were obtained in open capillary tubes and are not corrected. Elemental analyses were performed by MicroAnalysis, Wilmington, DE.

$\{CpCo(dppe)[P(OEt)_3]\}(BF_4)_2$. $[CpCo(dppe)I]I$ (1.000 g, 1.28 mmol) and $AgBF_4$ (0.4984 g, 2.56 mmol) were reacted in CH_3CN (100 mL) under N_2 at 25 °C. AgI was removed by filtration through Celite, and the resulting orange-red solution was treated with $P(OEt)_3$ (0.2124 g, 1.28 mmol, 0.22 mL). A slow color change to yellow-orange occurred in 8 h. Removal of solvent under reduced pressure (25 °C) gave a dark orange solid (0.6513 g, 60% yield; mp 118–119 °C dec). Anal. Calcd for $C_{40}H_{44}CoP_3O_3B_2F_8$: C, 53.50; H, 4.90. Found: C, 53.21; H, 4.85. ^1H NMR (acetone-d_6): δ 7.75 (b, m, Ph, 20 H), 6.14 (s, Cp, 5 H), 3.85 (q, $P(OCH_2CH_3)$, 6 H, $^3J_{HP}$ = 6.6 Hz), 3.40 (m, $P(CH_2)_2P$, 4 H), 1.18 (t, $P(OCH_2CH_3)$, 9 H, $^4J_{HP}$ = 5.0 Hz). $^{31}P\{^1H\}$ NMR (acetone-d_6): δ +81.19 (b, m, $P(OCH_2CH_3)$), +76.37 (d, dppe, $^2J_{PP}$ = 91.7 Hz).

$\{CpCo(dppe)[P(O)(OEt)_2]\}(BF_4)$. $P(OEt)_3$ (0.2161 g, 1.30 mmol, 0.224 mL) was added to $[CpCo(dppe)I]I$ (1.010 g, 1.30 mmol) in $CHCl_3$ (100 mL) at 25 °C. After 24 h, the solvent was removed under reduced pressure (35 °C), yielding a bronze solid, which was chromatographed on silica gel. Unreacted $[CpCo(dppe)I]I$ separated with $CHCl_3$ elution. CH_3CN removed a yellow band that was the desired compound (0.014 g, 11% yield; mp 178–179 °C). The yield was not improved significantly by refluxing. Anal. Calcd for $C_{35}H_{39}CoO_3P_3BF_4$: C, 53.46; H, 4.96. Found: C, 52.53; H, 5.06. ^1H NMR ($CDCl_3$): δ 7.65 (b, m, Ph, 20 H), 5.53 (s, Cp, 5 H), 3.69 and 3.48 (b, m, $P(OCH_2CH_3)$, 4 H), 2.89 and 2.72 (b, m, $P(CH_2)_2P$, 4 H), 0.786 (t, $P(OCH_2CH_3)$, 6 H, $^4J_{HP}$ = 7.58 Hz). $^{31}P\{^1H\}$ NMR ($CDCl_3$): δ +82.94 (m).

Spectra and Kinetic Studies. High-resolution ^1H and $^{31}P\{^1H\}$ NMR spectra were recorded on a Bruker WM-250 FT spectrometer. ^1H chemical shifts were referenced to Me_4Si (δ = 0.0 ppm) while $^{31}P\{^1H\}$ shifts are relative to 85% H_3PO_4 (external) with positive shifts being downfield. Variable-temperature ^1H NMR spectra were obtained by using a Bruker B-VT1000 controller calibrated (<±2 °C) with CH_3OH.

The essential details of the kinetic experiments are the same as those described previously.[5] Stock solutions of $[CpCo(dppe)X]BF_4$ were prepared in 2.0 mL of acetone-d_6 (1% Me_4Si) for X = I^- (0.0440 g, 0.060 mmol, 3.0×10^{-2} M), Br^- (0.0414 g, 0.060 mmol, 3.0×10^{-2} M), and Cl^- (0.0387 g, 0.060 mmol, 3.0×10^{-2} M). $P(OMe)_3$ (0.0148 g, 0.120 mmol, 6.0×10^{-2} M) and $P(OEt)_3$ (0.0167 g, 0.120 mmol, 6.0×10^{-2} M) were prepared in 2.0 mL of acetone-d_6 (1% Me_4Si).

A typical experiment involved the reaction of 0.20 mL (6.0×10^{-6} mol) of the desired complex, **1**, and 0.10 mL (6.0×10^{-6} mol) of $P(OMe)_3$ in a 5.0-mm NMR tube. Three experiments at various temperatures were conducted for each cobalt–halide complex at constant reactant stoichiometry. Kinetic information was extracted by least-squares methods. The integrated intensities from the NMR spectra were converted to concentration values by the use of the initial concentration and the spectrum at t = 0 s. The Arbuzov reaction involving $P(OEt)_3$ was studied in a like manner at 20 °C.

The reaction of $\{CpCo(dppe)[P(OMe)_3]\}(PF_6)_2$ with $[(C_4H_9)_4N]X$ (X^- = Cl^-, Br^-, I^-) allows the reaction to be analyzed by starting with **2**. Stock solutions of $\{CpCo(dppe)[P(OMe)_3]\}(PF_6)_2$ (0.0562 g, 0.060 mmol, 3.0×10^{-2} M) and $[(C_4H_9)_4N]X$, X^- = Cl^- (0.0085 g, 0.030 mmol, 3.0×10^{-2} M), Br^- (0.0097 g, 0.030 mmol, 3.0×10^{-2} M) and I^-(0.0111 g, 0.030 mmol, 3.0×10^{-2} M), were prepared in 2.0 mL of acetone-d_6 (1% Me_4Si), respectively. A typical reaction involved mixing 0.20 mL of the $\{CpCo(dppe)[P(OMe)_3]\}(PF_6)_2$ solution (6.0

(17) Thusius, D. *Inorg. Chem.* **1971**, *10*, 1106.
(18) Bao, Q.-B.; Landon, S. J.; Rheingold, A. L.; Haller, T. M.; Brill, T. B. *Inorg. Chem.*, in press.
(19) Heck, R. F. *Inorg. Chem.* **1965**, *4*, 855. King, R. B. *Inorg. Chem.* **1966**, *5*, 82.

$\times 10^{-6}$ mol) and 0.20 mL of the $[(C_4H_9)_4N]X$ solution at 20 °C and monitoring the reaction as a function of time.

Registry No. (1)(BF_4) (X = Cl), 89463-14-9; (1)(BF_4) (X = Br), 89463-16-1; (1)(BF_4) (X = I), 89463-28-5; (2)$(BF_4)_2$ (R = Et), 93110-30-6; (2)$(PF_6)_2$ (R = Me), 93110-31-7; (3)(BF_4) (R = Et), 93110-33-9; (3)(BF_4) (R = Me), 89463-23-0; $[(C_4H_9)_4N]Cl$, 6309-30-4; $[(C_4H_9)_4N]Br$, 1643-19-2; $[(C_4H_9)_4N]I$, 311-28-4; $P(OMe)_3$, 121-45-9; $P(OEt)_3$, 122-52-1; [CpCo(dppe)I]I, 32842-39-0; $AgBF_4$, 14104-20-2.

Contribution from the Department of Medicinal Chemistry, Hiroshima University School of Medicine, Kasumi, Hiroshima 734, Japan, and Department of Chemistry, College of General Education, Hirosaki University, Bunkyo, Hirosaki 036, Japan

Effects of Imide Anions and Axial Donors on the Stability and Oxidation Behavior of Square-Planar 13–15-Membered Macrocyclic Tetraamine Complexes of Nickel(II) and Copper(II)

EIICHI KIMURA,*[1a] TOHRU KOIKE,[1a] RYOSUKE MACHIDA,[1a] RIEKO NAGAI,[1a] and MUTSUO KODAMA[1b]

Received December 14, 1983

Potentiometric, electrochemical, spectrochemical, and electron spin resonance studies have revealed the structure, stability, and oxidation behavior of square-planar macrocyclic tetraamine complexes of nickel(II) and copper(II) containing a variety of ring sizes (13–15 membered), number (0–3) of imide anions, and extraplanar phenyl, pyridyl, and pyridine *N*-oxide substituents. Standard electrode potentials $E°$ range from 0.72 to 0.04 V (vs. SCE) for $Cu^{III,II}$–macrocycle complexes and from 0.98 to 0.50 V for $Ni^{III,II}$–macrocycle complexes in aqueous solutions. The replacement of neutral amine donors of 14-membered tetraamines (N_4) by one to three anionic imide donors successively lowers the $E°$ values by 0.2 V for copper, while the opposite effects were seen for nickel. Oxidation of Ni(II) complexes with an appended pyridyl donor yields five-coordinate Ni(III) species with the neutral N_4 and four-coordinate Ni(III) with the dianionic N_4. Oxidation of the Ni(II) and Cu(II) complexes of N_4 carrying a pyridine *N*-oxide tail is anomalously facile.

Introduction

The dioxo tetraamines **1**, **8**, and **17**, depicted in Chart I, possess novel ligand properties of saturated macrocyclic tetraamines (N_4) blended with oligopeptide features.[2-6] They accommodate certain metal ions (e.g. Cu^{2+}, Ni^{2+}, Co^{2+}) in the macrocyclic N_4 cavities with simultaneous dissociation of the two amide protons to afford 1:1 complexes generally designated as $[M^{II}H_{-2}L]^0$. Possible resonance stabilization of the resulting imide anions imposes strict N_4 coordinate arrangements for coplanarity, as is the case for tripeptide complexes.[7]

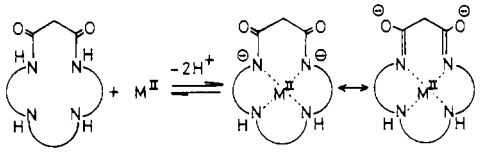

L square-planar $M^{II}H_{-2}L$

On the other hand, square-planar saturated and unsaturated N_4 ligands have been well demonstrated to stabilize various oxidation states of enclosed Fe,[8] Co,[9,10] or Ni[11,12] in aprotic solvents. The redox properties are determined by various structural parameters: a large ring, the presence of alkyl side chains to interfere with axial solvation, or unsaturation of N donors works for the lower valence states, while absence of these factors or the presence of negative charge on N donors stabilizes higher oxidation states.

Another efficient ligand factor facilitating higher oxidation states of metal ions in aqueous solutions was discovered in oligopeptide complexes of Cu(II)[13] and Ni(II),[14] where anionic imide N donors most dramatically reduce the electrode potentials $E°$ for $M^{III,II}$ couples, which successively decrease with an increase in the number of deprotonated peptide groups. Hence, highly deprotonated peptide complexes have extremely low potentials (e.g. $E° = 0.30$ V vs. SCE for the quadruply deprotonated *N*-formyltetraglycine complex of copper $CuH_{-4}L$) such that O_2 oxidation to M(III) may become thermodynamically feasible.[15] It is postulated that oxidative cleavage of peptides by air in the presence of Cu(II) or Ni(II) involves M(III)–peptide complexes as intermediates.

We have been devising simple macrocyclic ligands that produce proper ligand fields and steric environments so as to reproduce certain essential redox functions that occur in natural metal-containing enzymes. Therefore, our recent discovery[4] of the macrocyclic dioxo tetraamines **1**, **8**, and **17** has become highly significant in that they offer a new series of thermodynamically and kinetically efficient prototypes for generation of Cu(III) and Ni(III) in aqueous solutions. We report here the modification and extension of these new dioxo tetraamine structures by varying the number of amide functions and appending extraplanar potential donor functions in order to aim at better catalytic systems and mimic natural systems. Very recently,[5] we reported on novel macrocyclic dioxo pentaamine complexes of high-spin Ni(II) that possess a very low $E°$ value of 0.24 V vs. SCE and can activate O_2 by 1:1 Ni(II)–O_2 complexation so as to oxygenate benzene into phenol at room temperature.[5]

(1) (a) Hiroshima University. (b) Hirosaki University.
(2) Kodama, M.; Kimura, E. *J. Chem. Soc., Dalton Trans.* **1979**, 325.
(3) Kodama, M.; Kimura, E. *J. Chem. Soc., Dalton Trans.* **1979**, 1783.
(4) Kodama, M.; Kimura, E. *J. Chem. Soc., Dalton Trans.* **1981**, 694.
(5) Kimura, E.; Sakonaka, A.; Machida, R.; Kodama, M. *J. Am. Chem. Soc.* **1982**, *104*, 4255.
(6) Machida, R.; Kimura, E.; Kodama, M. *Inorg. Chem.* **1983**, *22*, 2055.
(7) Bossu, F. P.; Margerum, D. W. *J. Am. Chem. Soc.* **1976**, *98*, 4003. The free ligand **8** shows an infrared stretching frequency of the amide carbonyl at 1655 cm^{-1} (KBr pellet), while its copper(II) complex $CuH_{-2}L$ isolable as crystals displays this at 1580 cm^{-1}, supporting the resonance structures for the imide anion complexes.
(8) Herron, N.; Busch, D. H. *J. Am. Chem. Soc.* **1981**, *103*, 1236.
(9) Tait, A. M.; Lovecchio, F. V.; Busch, D. H. *Inorg. Chem.* **1977**, *16*, 2006.
(10) Hung, Y.; Martin, L. Y.; Jackels, S. C.; Tait, A. M.; Busch, D. H. *J. Am. Chem. Soc.* **1977**, *99*, 4029.
(11) Pillsbury, D. G.; Busch, D. H. *J. Am. Chem. Soc.* **1976**, *98*, 7836.
(12) Busch, D. H. *Acc. Chem. Res.* **1978**, *11*, 392.
(13) Bossu, F. P.; Chellappa, K. L.; Margerum, D. W. *J. Am. Chem. Soc.* **1977**, *99*, 2195.
(14) Bossu, F. P.; Margerum, D. W. *Inorg. Chem.* **1977**, *16*, 1210.
(15) Lappin, A. G.; Murray, C. K.; Margerum, D. W. *Inorg. Chem.* **1978**, *17*, 1630.

0020-1669/84/1323-4181$01.50/0